Orientational dependence of the tails of dipole-broadened NMR spectra in crystals

V. E. Zobov*) and Yu. N. Ivanov

L. V. Kirenskiĭ Institute of Physics Siberian Division, Russian Academy of Sciences, 660036 Krasnoyarsk, Russia

M. A. Popov

Krasnoyarsk State University, 660041 Krasnoyarsk, Russia

A. I. Livshits

Institute of Chemistry and Chemical Technology, Siberian Branch, Russian Academy of Sciences, 660036 Krasnoyarsk, Russia

(Submitted 3 July 1998)
Zh. Éksp. Teor. Fiz. **115**, 285–305 (January 1999)

This paper describes experimental and theoretical studies of the tails of the dipole-broadened nuclear magnetic resonance (NMR) absorption spectra of ^{19}F in isomorphic single crystals of BaF_2 and CaF_2 with the magnetic field directed along three crystallographic axes. The results obtained by directly measuring the derivative of the tail of the NMR absorption spectrum and the falloffs of the Engelsberg–Lowe free precession after Fourier transformation qualitatively agree. It is shown that the shape of the tail is well described by an exponential function in which the orientational dependence of the exponent does not reduce to variation of the second moment. The observed shape of the tail and the orientational dependence of its parameters are explained on the basis of a self-consistent fluctuating-local-field theory. Nonlinear integral equations are derived for the correlation functions, taking into account the changes of the actual number of nearest neighbors caused by the anisotropy of the dipole–dipole interaction and the contribution of lattice sums with loops. The equations are solved numerically. Good agreement is obtained for the computed dropoffs of the free precession, the NMR spectra, and the cross-polarization rates with the experimental results. © *1999 American Institute of Physics.* [S1063-7761(99)02401-4]

1. INTRODUCTION

The continued interest in the problem of the absorption line shape and the spectra of other correlation functions measured by nuclear magnetic resonance (NMR) in the solid state has two causes: first, the important applied significance of NMR for studying the properties of solids at the microlevel, and second, as a typical many-body problem. An indisputable advantage of model crystals such as CaF_2 or BaF_2 is the simplicity of the known laws governing the interactions in their nuclear magnetic subsystems (the main one of which is the dipole–dipole subsystem) and the possibility of experimentally verifying the theoretical derivations. The central part of the spectrum is ordinarily used in applied problems in this case, whereas information concerning the fundamental multiparticle dynamic properties of the system is included in the tails of the spectrum. This is because, in a homogeneous regular system, a response to an effect with a frequency many times as great as the rms precessional frequency in a local field is impossible unless a large number of spins participate. The distant region of the spectrum (the tail) is of the greatest practical interest when one is studying processes involving the establishment of equilibrium in a spin system consisting of strongly differing resonance frequencies of the subsystems (the reservoirs)—cross-relaxation processes. This is shown by the large number of experimental papers on measuring the rates of these processes (see the citations and their analyses in Ref. 1). The study of such processes in turn is closely associated with the general problem of mixing in nonlinear mechanics.

Because of this multifrequency behavior, calculation of the tails of the spectra of the correlation functions imposes requirements on the theory unlike those of the calculation of the central part. It is very difficult to experimentally measure the tails, because they are small and are therefore strongly affected by noise, nonideal properties of the apparatus, etc. For these reasons, the tails of the spectra have been insufficiently studied both theoretically and experimentally. This is also very true for the tails of the NMR absorption line. The experimental papers we are aware of measured either the central part or the Fourier transform—the falloff of the free precession. The former relates to the work of Bruce,[2] and the latter to that of Engelsberg and Lowe,[3] which is of tremendous interest among theoreticians because of the oscillations of the falloff of the free precession in CaF_2, measured with high accuracy. In fact, it became the cornerstone of theories concerning the NMR line shape (see, for example, Refs. 4–10).

The exponential form of the tail of the NMR spectrum follows from the results of Ref. 3 (see Appendix A), and this agrees with the results of a number of experiments[1,11–14] and

TABLE I. Parameters of the NMR spectrum of ^{19}F in BaF_2 for three directions of the magnetic field.

Field direction	M_2^{theor}, Oe^2	M_2^{exp}, Oe^2	$2H_m$, Oe	N_s	S_3/S_1^2	K_6	K_8
[111]	1.055	1.219	0.4	25	0.12	0.10	0.4
[110]	2.284	2.324	0.5	20	0.17	0.18	0.5
[100]	5.966	5.798	0.6	12	0.09	0.05	0

of the theory constructed in the approximation of a self-consistent fluctuating field.[15–19] Other papers on the theory of the line shape did not pay proper attention to the tail. Thus, for example, it falls off more quickly in the constant-local-field approximation[4,5] than for a Gaussian function, whereas, when the field fluctuations are specified by a random Markov process,[7,10] the tail becomes a power function. In the theory that we developed,[16–18] in which the approximation of a self-consistent fluctuating field is chosen, corresponding to the limit of systems of large dimensionality, all the parameters are expressed in terms of one scale parameter, the second moment. However, the variations of the parameters of the tails of the spectra of the experimental falloffs of the free precession in Ref. 3 are not described by the variation of only the second moment when the magnetic field is directed along the crystallographic axes [100], [110], and [111].

This paper derives nonlinear integral equations for the correlation functions in the self-consistent fluctuating-local-field approximation,[1,16–19] taking into account the characteristics of actual lattices, which, as a consequence of the anisotropy of the dipole–dipole interaction, depend on the magnetic-field orientation. At the same time, this paper reports the direct measurement of the tail of the NMR absorption line of ^{19}F in a BaF_2 crystal isomorphous with CaF_2, with the same magnetic-field directions. Such an experiment seems important to us, since the fraction of high frequencies in the spectrum is exponentially small, and they can easily be distorted during observation in the dropoff of the free precession in a mixture with the central part of the spectrum. The orientational dependences of the parameters of the tail, measured by two methods, are in qualitative agreement. These results are explained from the position of the theory that we developed.

2. EXPERIMENT

The single crystal of BaF_2 studied here was grown at the Crystallography Institute, Russian Academy of Sciences, by the Bridgman method. The quality of the crystal was monitored by x-ray phase analysis and by NMR. The long spin-lattice relaxation time is evidence that the concentration of paramagnetic impurities in the test sample is low. The single crystal was oriented on an x-ray diffractometer. The lattice parameter of 6.2001 Å in BaF_2 (Ref. 20) is a factor of 1.14 greater than in CaF_2. The experiment was run on a modified RYa-2310 spectrometer with an autodyne sensor in a 12-kOe field at room temperature. The first derivative of the NMR absorption line was digitally measured by a microprocessor device with field scanning of the spectrum. The long-term stability of the spectrometer parameters was monitored by simultaneously measuring the signal from a mark placed in part of the coil of the NMR sensor separately from the sample. Particular attention was paid to choosing the optimum rf field so that the saturation effect was below the noise level. The SNR was substantial increased by accumulating the NMR signal by multiple scanning of the spectrum (the number N_s of scans is shown in Table I). The time for one scan was 20 min.

The NMR lines were measured with a constant magnetic field oriented along the crystallographic axes. Because the spectra are symmetric, Fig. 1a shows only half of them. Figure 1b shows the tails of these derivatives on a semi-log plot. The curves in the figures are normalized to unit area of the absorption line. The deviation of the field from the center of the spectrum in each orientation is expressed in units of $M_2^{1/2}$, where M_2 is the second moment of the spectrum. This eliminates the difference of the scales of the spectra and allows their shapes to be compared.

The experimental values of M_2 were calculated by extrapolating the ratio of the integrals of the product of the measured first derivatives of the spectrum and the cube of the detuning and the triple detuning to larger values of the upper limit of integration.[21] Table I also shows the theoretical values of the second moments for BaF_2. The latter were calculated using lattice sums from Refs. 12 and 22, taking into account the small contribution of the magnetic isotopes ^{135}Ba and ^{137}Ba, whose maximum is reached in the [111] orientation and equals 3% of the contribution of the ^{19}F nuclei. Moreover, because the NMR line is broadened by modulating the constant magnetic field with an amplitude of H_m (see Table I), $H_m^2/4$ should be added to these values of the second moment.[23] The remaining differences of the theoretical and experimental values of the moments are associated with imprecision in the orientation of the crystal in the magnetic field. Since we consider spectra normalized to M_2, a slight discrepancy of the moments does not prevent the shapes of the spectra from being compared. Therefore, we shall pay no attention to these differences in what follows, nor to the contribution of the Ba nuclei and the field modulation to the broadening. According to our estimates, the possible shape distortions of the tail are below the experimental accuracy.

Figures 1a and 1b also show the derivatives of the spectra obtained by Fourier-transforming the function

$$f(t)=\exp\{C[A-(A^2+t^2)^{1/2}]\}\prod_{n=1}^{61}(1-\alpha_n^2t^2), \qquad (1)$$

which Engelberg and Lowe[3] used to accurately describe their experimental dropoffs of the free precession in CaF_2. They determined the parameters which determine this function for the same three magnetic field orientations. When the curves

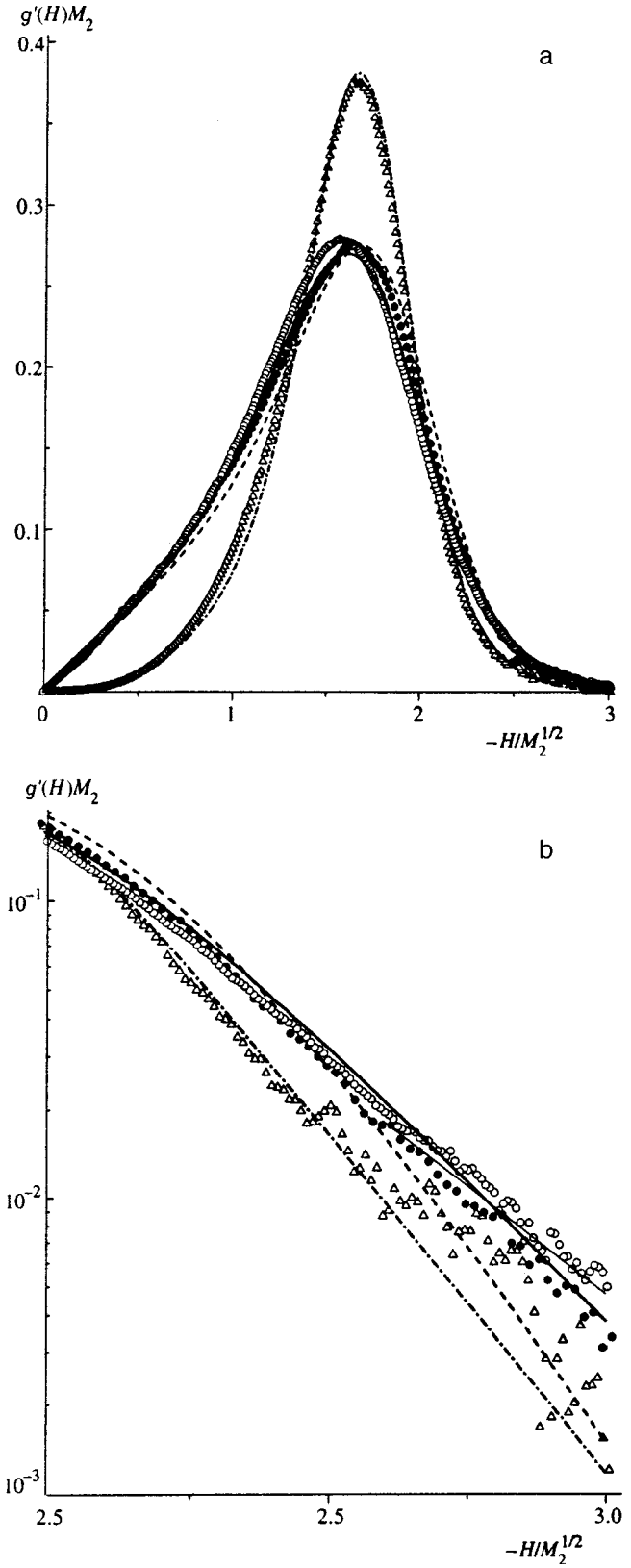

FIG. 1. Derivatives of the NMR absorption spectra of ^{19}F in BaF_2 [(a) central part, (b) tail] as a function of the detuning from the center of the spectrum, with the magnetic field directions along the crystallographic axes [100] (triangles), [110] (closed circles), and [111] (open circles). The dot-dashed, dashed, and solid curves show the derivatives of the Fourier spectra of the Engelsberg–Lowe function, Eq. (1), in the corresponding orientations. A thin line segment is drawn in (b) according to the asymptotic formula, Eq. (2). All the curves are normalized to unit area of the absorption spectrum and unit second moment.

in the figure were calculated, these parameters were expressed in units of the experimental values of the second moments for CaF_2 given in this paper. It can be seen from the figure that the Fourier transform of the function given by Eq. (1) generally describes our experimental NMR absorption spectrum. The small differences can be associated with the noncoincidence of the orientations of the crystals and the instrumental functions of the two methods.[24,25] together with the replacement of the actual falloffs of the free precession in Ref.3 by the simple function given by Eq. (1). We shall return to this question below.

We proceed to an analysis of the shape of the tail of the NMR spectrum. To describe it, we turn to the theory that we developed,[1,16–19] based on the self-consistent fluctuating-local-field approximation, by means of which, in the limit $H \gg M_2^{1/2}$ (the H field is measured from the center of the spectrum), the desired tail is determined from

$$g(H) \simeq c_0 |H|^{\chi} \exp(-|H|\tau_0), \tag{2}$$

where τ_0 is the coordinate of the closest two singular points, symmetrically placed relative to the coordinate origin on the imaginary time axis, and c_0 and χ are characteristics of the singular points. In the limit of a large number of nearest neighbors,[16,17]

$$\tau_0 = 3.72/M_2^{1/2}, \quad c_0 \approx 29.3 M_2, \quad \chi = 1. \tag{3}$$

A section of the curve corresponding to the derivative of Eq. (2) is shown in Fig. 1b. It passes fairly close to the experimental tail in the [111] orientation. In the other two orientations, the tails of the experimental spectra fall more steeply.

We now turn to the Engelsberg–Lowe function given by Eq. (1). As can be seen from Fig. 1b, its spectrum decreases more quickly in all three orientations. The asymptotic expression for the tail of the spectrum of this function, obtained in Appendix A, has the form of Eq. (2) with $\chi = -1/2$ and $\tau_0 = A$. An unexpected orientational dependence is detected in the exponential in this case: A is larger in the [110] orientation than in the [100] orientation.

Our analysis of the curves in Fig. 1b thus shows that, first, the shape of the spectrum at the tail is close to exponential, given by a straight line in the semi-log coordinates chosen in the figure. Second, the slope of the corresponding straight lines depends on the orientation of the crystal in the magnetic field. Since the change in the width of the spectrum with orientation is already taken into account in Fig. 1b after transforming to dimensionless fields measured in units of $M_2^{1/2}$, the remaining change of the slope of the straight lines is evidence of an additional orientational dependence of the argument of the exponential.

3. THEORY

To explain the observed orientational dependence of the tail of the NMR spectrum, let us consider the system of spins ($I = 1/2$) of the ^{19}F nuclei of the fluorite crystal, which form a simple cubic lattice. We write the Hamiltonian of the secular part of the dipole–dipole interaction in a strong constant magnetic field[25] as

$$\mathscr{H}_d = \sum_{i \neq j} b_{ij}[I_i^z I_j^z - \xi(I_i^x I_j^x + I_i^y I_j^y)], \tag{4}$$

where $b_{ij} = \gamma^2\hbar[1-3\cos^2\theta_{ij}]/2r_{ij}^3$, θ_{ij} is the angle made by the internuclear vector $\mathbf{r}_{ij}$ with the constant magnetic field $\mathbf{H}_0$, and $\xi = 1/2$ is a parameter that we introduced for convenience in the theoretical analysis. We shall describe the dynamics of the spin system by the correlation functions

$$\Gamma_p(t) = \mathrm{Tr}\{\exp(i\mathscr{H}_d t) I_p \exp(-i\mathscr{H}_d t) I_p\}/\mathrm{Tr}\{(I_p)^2\}, \tag{5}$$

where the subscript $p = 1,2,3$ indicates the three correlation functions: $\Gamma_1(t) = M_x(t)$ is the correlation function of the x projection of the total spin of the system or the transverse component of the magnetization, coinciding with the falloff of the free precession; $\Gamma_2(t) = \Gamma_x(t)$ and $\Gamma_3(t) = \Gamma_z(t)$ are the autocorrelation functions of the x and z components of an individual spin of the system, respectively.

In the self-consistent fluctuating-local-field approximation, corresponding to the limit $d \to \infty$, the system of equations for the correlation functions (4) is obtained in the form[16–18]

$$\frac{d}{dt}\Gamma_p(t) = -\int_0^t G_p(t-t')\Gamma_p(t')dt'. \tag{6}$$

The kernels $G_p(t)$ of the integral equations (the memory functions) can be represented as a series over irreducible dressed skeletal diagrams, each term of which is expressed via a multiple time integral of the products of the functions $\Gamma_x(t')$ and $\Gamma_z(t'')$. As shown in Refs. 16 and 17, the equations for the autocorrelation functions are the equations for the precession of the magnetic moment in a three-dimensional Gaussian random local field. These equations have a complex form because the rotations around the time-varying instantaneous field directions are noncommutative. In this approximation, all the coefficients in $G_p(t)$ are expressed in terms of M_2, and therefore, in the solutions of the equations, the orientational dependence repeats the dependence of M_2 and reduces to a variation of the time scale in Eqs. (5).

For three-dimensional lattices, Refs. 15, 26, and 27 proposed to introduce correction terms in the kernel $G_p(t)$, the number of which rapidly increases as the number of vertices on the diagrams increases. Such an equation is hard to use in practice. It is necessary to regroup the series for the kernel so that its first several terms are sufficient to describe the experiments.

To do this, we separate out from the dipole–dipole interaction of Eq. (4) the longitudinal part, consisting of the spin components parallel to the external constant magnetic field.[1,4–6,8,10,18,27] Although the coefficients of the two parts in Eq. (4) differ by only a factor of two, the longitudinal part is distinguished by the axial symmetry of the Hamiltonian, which causes the projection of the total spin onto the z axis to be conserved in time. It is also important that for $\xi = 0$ the autocorrelation function given by Eq. (5) for the x projection of spin i is easy to compute:[4,25]

$$\Gamma_0(t) = \prod_j \cos(b_{ij}t), \tag{7}$$

and describes the independent precession of one of the spins of the system in its constant longitudinal local field, $2\Sigma_j b_{ij} I_j^z$.

The transverse part of the interaction given by Eq. (4), consisting of the spin components perpendicular to the external constant magnetic field, as is well known,[25] plays an important role in transporting polarization from node to node (spin diffusion). Taking into account the transport of the transverse polarization, Refs. 4 and 5 derived an equation in first order in the transverse interaction:

$$M_x(t) = \Gamma_\lambda(t) + K\int_0^t \frac{d\Gamma_\lambda(t')}{dt'} M_x(t-t')dt', \tag{8}$$

where

$$K = 9/4\lambda^2 - 1, \tag{9}$$

and $\Gamma_\lambda(t)$ is the correlation function given by Eq. (7) with coefficient b_{ij} increased by factor of λ. This equation, which we shall call the basic approximate equation, gave a good description of the falloff of the free precession in CaF_2 for $\lambda = 1.225$ (Ref. 4) and $\lambda = 1.19$.[5] Note that the factor λ in Refs. 4–6 and 16 has a different physical basis. We shall regard it as a renormalization parameter of the longitudinal local field, defined in terms of the moment of the spectrum.

The success of Eq. (8) in describing the falloff of the free precession suggests that, after the terms in Eq. (6) corresponding to Eq. (8) are singled out, the rest of the series for the kernel will play the role of a small correction. We carry out the indicated transformation by the following formal procedure. We represent $\Gamma_\lambda(t)$ as the solution of an integral equation of the form (6) with kernel $Q(t)$, which can be given by series $G_2(t)$ if the terms with vertices corresponding to interaction between transverse spin projections are discarded from it. By combining the Laplace transforms of this equation and Eqs. (6) and (8), we find

$$M_x(t) = \Gamma_\lambda(t) + K\int_0^t \frac{d\Gamma_\lambda(t')}{dt'} M_x(t-t')dt' - \int_0^t \Phi(t-t')M_x(t')dt', \tag{10}$$

where

$$\Phi(t) = \int_0^t \Gamma_\lambda(t-t')\{G_1(t') - (1+K)Q(t')\}dt'.$$

The resulting equation makes it possible to find the necessary correction terms, since it is formally exact when the complete series for $G_1(t)$ and $Q(t)$ are retained.

Another important consequence of the transverse interaction is the time variation of the spin orientation, which causes I_j^z to be replaced by $I_j^z(t)$ in the expression for the longitudinal local field. The basic approximate Eq. (8) does not reflect such fluctuations, whose presence follows not only from theory but also from experiments, for example, from the cross-polarization of the rare nuclei ^{43}Ca,[11] in which the spectrum of these fluctuations is measured. Therefore, although the falloff of the free precession is successfully described by this equation at short times, discrepancies

with experiment appear at long times. In particular, beats appear in the oscillations of the falloff of the free precession and are especially appreciable in the [100] orientation in the region of the 5–7th zeros.[4] The tails of the Fourier spectra decrease more rapidly in the calculated falloffs of the free precession than with Gaussian functions.

We will include fluctuations of the longitudinal local field in the basic approximate equation (8), having replaced $\Gamma_\lambda(t)$ with a new autocorrelation function $P(t)$. The procedure for deriving Eq. (10) allows us to make such a replacement in this equation. To determine $P(t)$, we consider the correlation function of the longitudinal local field at spin i,[16,17]

$$2\lambda\sum_j b_{ij}I_j^z(t).$$

Interaction with this spin is excluded in the time evolution of its neighboring spins:

$$\langle\omega_i(t)\omega_i\rangle=\lambda^2\sum_j b_{ij}^2\Gamma_{zj/i}(t)+\lambda^2\sum_{j,k} b_{ij}b_{ik}\Gamma_{zjk/i}(t). \tag{11}$$

The first term contains the autocorrelation function of the z projection of spin j. The second term is the overlap correlation function of the two spins j and k. The slash indicates that interaction with the selected spin i is excluded, as mentioned above. The contributions to the local field from the different spins of the neighborhood are not independent. Such independence appears only in the limit $d\to\infty$.[1,16,17] In fact, in this limit, lattice sums with loops composed of bonds become negligible by comparison with lattice sums that contain no loops and that are expressed in terms of the power of the second moment. Other model systems where there are no loops are systems on Bethe lattices.[19] The contributions of adjacent spins to the local field will also be independent in these systems, since interaction with spin i is excluded in them. Bethe lattices have an advantage over hypercubic lattices of infinite dimensionality in that the number Z of neighbors in them can be arbitrary.

The contribution of the second term in Eq. (11) is comparatively small for a cubic lattice, although it does not disappear. To estimate it, we expand Eq. (11) in powers of time:

$$\langle\omega_i(t)\omega_i\rangle=\lambda^2S_1+2\xi^2\lambda^4S_1^2(1-S_2/S_1^2-S_3/S_1^2)t^2+O(t^4), \tag{12}$$

where

$$S_1=\sum_j b_{ij}^2,\quad S_2=\sum_j b_{ij}^4,\quad S_3=\sum_{j,k} b_{ij}b_{ik}b_{jk}^2 \tag{13}$$

are known lattice sums.[12,22] The term with S_2 in Eq. (12) results from excluding interaction with the selected spin, while the term with S_3 characterizes the correlation of the contributions. The ratio S_3/S_1^2 in a cubic lattice varies from 0.17 in a [110] orientation to 0.09 in a [100] orientation.

It follows from Eq. (12) that correlation in the motion of the spins that create the local field weakens its fluctuations. The same conclusion can be drawn from the expression for the correlation function of the local field of a heteronuclear system proposed in Ref. 28. This paper, besides the expansion for short times, treated the diffusion asymptotics of the autocorrelation function of the field as $t\to\infty$. We do not do this, because the spectral tail of interest to us is determined by the singular points on a comparatively small time interval from the beginning, and diffusion can not develop. Neglecting diffusion tails allows us to write for Eq. (11) the following expression, which is simpler than that in Ref. 28:

$$\langle\omega_i(t)\omega_i\rangle=\lambda^2\sum_j b_{ij}^2\Gamma_{zj/i}^\nu(t), \tag{14}$$

where the attenuation of the fluctuations indicated above is introduced via the exponent $\nu<1$. In particular, when

$$\nu=\nu_0\equiv 1-S_3/S_1^2,$$

the first two terms of the time expansion of Eq. (14) coincide with Eq. (12). At long times, additional attenuation of the fluctuations from more complicated loops should be expected, as well as bulk interaction of the branches of the trees formed by the b_{ij} bonds.[19] An estimate of the latter for the Heisenberg model by numerical modelling of the placement of the trees on a cubic lattice gave $\nu=\nu'\approx 2/3$.[19] If this value of ν' is used and both these effects are taken into account, the index $\nu=\nu'\nu_0$ changes from 0.55 to 0.61 in different orientations. Bearing in mind that this is a rough estimate, we shall set $\nu=1/2$ in subsequent calculations.

The main advantage of the approximation given by Eq. (14) is that it keeps the contributions of different spins to the longitudinal local field independent when the fluctuations of the latter are taken into account. Such an approximation makes it possible to obtain equations that are simple enough to be used in practice. As a result,

$$\Gamma_{xi}(t)\approx\left\langle\exp\left[2i\lambda\sum_j b_{ij}\int_0^t I_j^z(t')dt'\right]\right\rangle$$
$$=\prod_j\left\langle\exp\left[2i\lambda b_{ij}\int_0^t I_j^z(t')dt'\right]\right\rangle,$$

and the product of cosines in Eq. (7) is replaced by the product

$$P_i(t)=\prod_j F_{ij}(t) \tag{15}$$

of functions that satisfy the equations

$$\frac{d}{dt}F_{ij}(t)=-\int_0^t G_{Fij}(t')F_{ij}(t-t')dt'. \tag{16}$$

The memory function in Eq. (16) can be determined as a series, as was done in Eq. (6). The first term of this series,

$$G_{Fij}^{(1)}(t)=\lambda^2b_{ij}^2\Gamma_{zj/i}^\nu(t) \tag{17}$$

is the contribution to Eq. (14) from spin j. The appearance of the remaining terms of the series is associated with the noncoincidence of the correlation function of the product of the operators

$$\prod_{p=1}^{2n} I_j^z(t_p)$$

with the product of the two-spin correlation functions. In the basic approximate equation, we restrict ourselves to the first term of this series, Eq. (17). Its remaining part is implied in the correction given by Eq. (10). As is to be expected, when the fluctuations are neglected [for $\Gamma_{zj/i}(t)=1$], Eq. (15) gives a product of cosines, Eq. (7), whereas, in the limit of a large number of neighbors, Eqs. (15)–(17) transform into an expression for $\Gamma_{xi}(t)$ with a Gaussian random field.[15–19,25,29]

An autocorrelation function $P(t)$ that takes into account the fluctuations of the longitudinal local field is thereby obtained. We next need to derive an equation for autocorrelation function $\Gamma_{zj/i}(t)$. We take Eq. (6) for the corresponding function, while keeping only the first term in the series for its kernel[1,16,17,26,27] [we recall that the remaining part of this series is meant to be treated as correction terms of Eq. (10)]:

$$\frac{d}{dt}\Gamma_{zj}(t)=-2\xi^2\sum_k b_{jk}^2\int_0^t\Gamma_{xj}(t')\Gamma_{xk}(t')\Gamma_{zj}(t-t')dt'. \tag{18}$$

To clarify the subsequent transformations, we have written out the nodal indices of the interacting spins in Eq. (18). As pointed out above, the equation has such a form in the limit of a large number of neighbors. When the number of neighbors is limited, it becomes important to exclude from the autocorrelation functions the interaction with spins already explicitly included via b_{jk}^2. Carrying out such a procedure and replacing $\Gamma_{xj}(t)$ with $P_j(t)$, we obtain

$$\frac{d}{dt}\Gamma_{zj/i}(t)=-2\xi^2\sum_{k(\neq i)} b_{jk}^2\int_0^t P_{j/ik}(t')\times P_{k/ij}(t')\Gamma_{zj/i}(t-t')dt', \tag{19}$$

where we recall that the indices of the spins with which interaction is excluded are shown after a slash in the symbols of the functions.

The system of Eqs. (15)–(17) and (19) determines the desired autocorrelation functions self-consistently. If function $P(t)$ is then substituted into Eq. (8) in place of $\Gamma_\lambda(t)$, we get the basic approximate equation for $M_x(t)$, taking into account the fluctuations of the longitudinal fields. For the first two moments of the NMR spectrum [the coefficients of the expansion of $M_x(t)$ in powers of time], we get from these equations

$$M_2=(1+K)\lambda^2 S_1,$$
$$\frac{M_4}{M_2^2}=1+\frac{2}{1+K}\left(1+\frac{\nu\xi^2}{\lambda^2}\right)-2\left(1+\frac{\nu\xi^2}{\lambda^2}\right)\frac{S_2}{(1+K)S_1^2}. \tag{20}$$

This result should be compared with the exact expressions for the moments:[25,30]

$$M_2=(1+\xi)^2 S_1,$$
$$\frac{M_4}{M_2^2}=3-B-\frac{(2-B)S_2}{S_1^2}+\frac{BS_3}{S_1^2}, \tag{21}$$
$$B=\frac{4\xi}{1+\xi}-\frac{6\xi^2}{(1+\xi)^2}.$$

Comparing the expressions for M_2, we find that

$$K=(1+\xi)^2/\lambda^2-1,$$

which transforms into Eq. (9) when $\xi=1/2$. Equating the coefficients in front of the lattice sums for M_4 in Eqs. (20), we find

$$\nu=(1+2\xi^2-\lambda^2)/\xi^2. \tag{22}$$

In particular, the values $\nu=1/2$ and $\xi=1/2$ correspond to $\lambda^2=11/8$.

To restore the missing contribution from S_3 in Eqs. (20) for M_4, we go overfrom Eq. (8) to Eq. (10), replace $\Gamma_\lambda(t)$ in it by $P(t)$, and write correction $\Phi(t)$ in the form

$$\Phi_4(t)=\frac{3BS_3M_2}{4S_1^2\lambda^2}\int_0^t\varphi(t-t')\Gamma_z^\nu(t')\{\dot P(t-t')\times P(t')+P(t-t')\dot P(t')\}dt', \tag{23}$$

where

$$\varphi(t)=\int_0^t\Gamma_z^\nu(t')dt',\quad \dot P(t)=\frac{dP(t)}{dt},$$

while the correlation functions under the integral are determined without limitations on the interaction. For clarity, we show this correction in the diagram representation of Refs. 16–18:

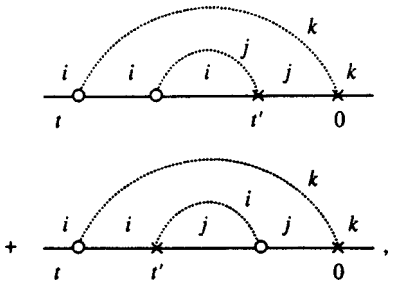

(24)

where $\times$ indicates a transverse vertex and $\bigcirc$ indicates a longitudinal one, and the lines show the autocorrelation functions of spins i, j and k (the x projections are shown by solid curves, and the z projections by dotted curves). Let us turn our attention to the approximate replacement $\Gamma_z^\nu(t'')\approx\Gamma_z^\nu(t''-t')\Gamma_z^\nu(t')$, made when we go from Eq. (24) to Eq. (23) to simplify the calculations. The two successive diagrams with two vertices already taken into account in Eq. (8),

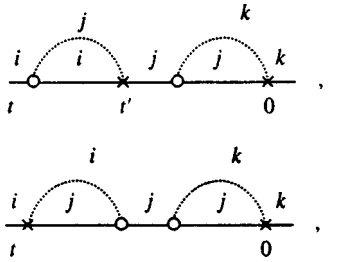

(25)

differ from $\Phi_4(t)$ in Eq. (24) in the placement of the vertices. The physical meaning of Eq. (24) is that the polarization can be transferred from spin i to spin k not only via the two-spin correlations given by Eq. (25) but also via three-spin correlations that have the form of a loop composed of bonds and therefore do not reduce to the square of the two-spin correlations. Function $\Phi(t)$ also contains diagrams with another placement of four vertices. To simplify the equations, we do not exhibit all of them, since they have the same qualitative effect as those already shown, and their contribution was taken into account by the choice of the coefficient in Eq. (23).

Besides four-vertex corrections, $\Phi(t)$ contains corrections with a larger number of vertices. Since they have a weaker role, to simplify the calculations we take them in simpler form than in $\Phi_4(t)$:

$$\Phi_{2n}(t)=K_{2n}D_n(t), \tag{26}$$

$$D_n(t)=\int_0^t dt_1\dot{P}(t-t_1)\Gamma_z^{\nu}(t_1)D_{n-1}(t_1), \quad D_1(t)=\dot{P}(t). \tag{27}$$

We choose the coefficients K_{2n} for $n>2$ by fitting $M_x(t)$ to the experimental dropoffs of the free precession.

4. CALCULATION AND DISCUSSION

The system of Eqs. (15)–(17) and (19) consists of an enormous number of nonlinear equations, which makes it hard to solve. Fortunately, the main contribution to the determination of the form of the spectrum comes from the interaction with a comparatively small number Z of nearest neighbors.[6,9] Thus, in the case of CaF_2 and BaF_2, we choose $Z=20$ when a strong constant magnetic field is along the [111] crystallographic axis, $Z=8$ when it is along [110], and $Z=6$ when it is along [100]. This variation of Z results from the strong anisotropy of the dipole interaction constants of the magnetic moments of the fluorine nuclei.[6,9] Because of the symmetry of the field orientations considered here, the interaction constants with the Z chosen neighbors take no more than three values. We denote the three corresponding coefficients b_{ij}^2 in Eqs. (17) and (19) as b_q ($q=1,2,3$) and express them in units of M_2. We denote the number of neighbors with interaction coefficient b_q as n_q. For the [100] orientation we get

$$b_1=d_c/27, \quad b_2=4b_1,$$

$$n_1=4, \quad n_2=2, \quad d_c=0.898,$$

for the [110] orientation we get

$$b_1=d_c/36, \quad b_2=4b_1, \quad b_3=2b_1,$$

$$n_1=4, \quad n_2=n_3=2, \quad d_c=0.791,$$

and for the [111] orientation we get

$$b_1=4m/9, \quad b_2=4m, \quad b_3=27m/8,$$

$$n_1=6, \quad n_2=2, \quad n_3=12, \quad m=8d_c/921, \quad d_c=0.825.$$

The ratio of the contribution from the remaining Z neighbors to the total second moment—the constant d_c—was determined by means of the lattice sums from Ref. 12.

Keeping only these interactions in Eqs. (15)–(17) and (19) and taking $\xi=1/2$, we get the following system of nonlinear equations for the autocorrelation functions:

$$\frac{d}{dt}F_q(t)=-\lambda^2 b_q\int_0^t\Gamma_{z/q}^{\nu}(t-t')F_q(t')dt', \tag{28}$$

$$\frac{d}{dt}\Gamma_{z/q}(t)=-\frac{1}{2}\int_0^t\Gamma_{z/q}(t-t')\left\{\frac{b_1n_1}{F_1^2(t')}+\frac{b_2n_2}{F_2^2(t')}+\frac{b_3n_3}{F_3^2(t')}-\frac{b_q}{F_q^2(t')}\right\}\frac{R_c^2(t')dt'}{F_q(t')}, \tag{29}$$

where

$$R_c(t)=F_1^{n_1}(t)F_2^{n_2}(t)F_3^{n_3}(t). \tag{30}$$

At the same time, Eq. (10) for the correlation function of the x projection of the total spin takes the form

$$M_x(t)=P(t)+K\int_0^t\frac{dP(t')}{dt'}M_x(t-t')dt'-\int_0^t\Phi(t-t')M_x(t')dt', \tag{31}$$

where

$$\Phi(t)=\sum_{n=2}\Phi_{2n}(t), \tag{32}$$

$$P(t)=R_c(t)R_f(t). \tag{33}$$

In Eq. (33), we have combined the contribution of a large number of distant spins in the form of the autocorrelation function of the spin in a random Gaussian field:

$$R_f(t)=\exp\left\{-\frac{4}{9}\lambda^2(1-d_c)\int_0^t(t-t')\Gamma_z^{\nu}(t')dt'\right\}, \tag{34}$$

where $\Gamma_z(t)$ is determined from an equation that differs from Eq. (29) in having A kernel does not contain the divisor $F_q(t)$ and the subtrahend $b_q/F_q^2(t)$. Finally, in Eq. (32) we determine $\Phi_4(t)$ from Eq. (23), and $\Phi_{2n}(t)$ with $n>2$ from Eq. (26).

Applying to the system of nonlinear equations (28) and (29) the same analysis methods as in Refs. 1 and 16–19, it can be shown that its solution has singular points on the imaginary time axis (see Appendix B). Consequently, the Fourier spectrum of this solution has exponential high-frequency asymptotics determined by the nearest singular points. Since the detunings achieved in experiment are not large enough for us to limit ourselves to the first term of the asymptotic series, we shall not dwell on an analysis of the singular points but immediately proceed to a numerical solution of the resulting equations.

The system of Eqs. (28)–(31) was solved by the method of finite differences. The falloffs of the free precession were accurately calculated on the time interval from $t=0$ to

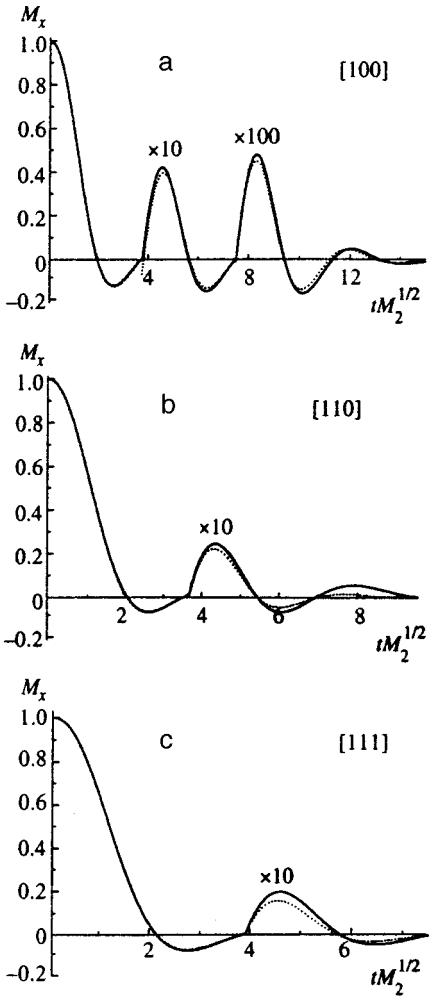

FIG. 2. Falloffs of the free precession $M_x(t)$ with the magnetic field directions along the crystallographic axes [100] (a), [110] (b), and [111] (c), increased at long times by factors of 10 and 100. The solid curves are the theoretical results, and the dashed curves are the Engelsberg–Lowe functions, Eq. (1).

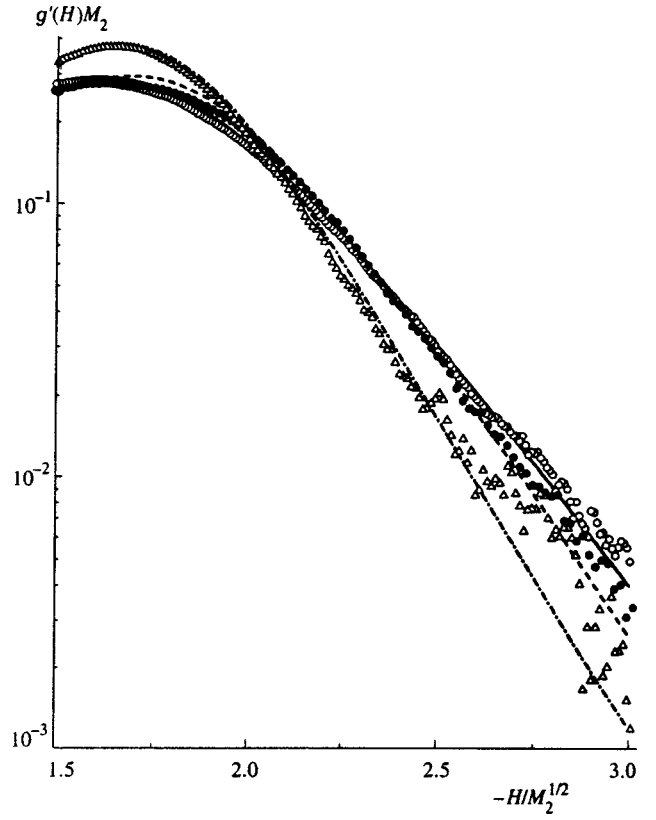

FIG. 3. Tails of the derivatives of the Fourier spectra of the theoretical curves shown in Fig. 2, in comparison with the experimental tails of the NMR absorption spectra of ^{19}F in BaF_2 shown in Fig. 1. The theoretical curves are solid for the [111] orientation, dashed for [110], and dot–dashed for [100].

$t=20M_z^{-1/2}$, broken up into 2000 points. The results are shown in Fig. 2, while the derivatives of their Fourier spectra are shown in Fig. 3. The calculation uses $\lambda^2=11/8$, $\nu=1/2$, and the values of the orientation-dependent parameters shown in Table I. A numerical analysis showed that the basic approximate equation without corrections gives oscillating falloffs of the free precession with an oscillation frequency less than the experimental value. The addition of $\Phi_4(t)$ increases the oscillation frequency, but excessively raises the amplitude of the first maximum (between the second and the third zeros). The correction $\Phi_6(t)$ made it possible to correct this distortion. The correction $\Phi_8(t)$ was also included in the [110] and [111] orientations, since the role of the complex correlations in the transfer of polarization is large in these orientations. This is reflected on the experimental falloffs of the free precession, in particular, in the inequivalence of the zeros (their approximation). One basic approximate equation gives the falloff of the free precession with equidistant zeros and a rapidly damped amplitude. Agreement with experiment can be achieved only by adding correction terms. In particular, the difference remaining at long times in Fig. 2b can be eliminated by adding $\Phi_{10}(t)$. Since the authors of Refs. 4–6 and 10 neglected polarization transfer via complex correlations and restricted themselves to the basic approximate equation, the calculated falloffs of the free precession that they obtained shows significantly worse agreement with experiment in these orientations.

Let us proceed to the results for the tail of the NMR spectrum. As can be seen from Fig. 3, the approximation chosen to describe the local-field fluctuations and expressed in Eqs. (28) and (29) correctly describes the shape of the tail and its orientational dependence. It follows from this that the damping of the tail speeds up as one goes from field orientation [111] to [110] and then to [100] mainly because the number Z of neighbors decreases. This can be explained qualitatively by noting that the field is created by Z neighbors, but it varies because of the interaction with the $Z-1$ spins. In the self-consistent approach this occurs each time more new spins are involved in the interaction with the passing of time. Consequently, the ratio for the higher-order moments can be expected to be

$$M_{2n}(Z)/[M_2(Z)]^n \sim M_{2n}(\infty)/[M_2(\infty)]^n[(Z-1)/Z]^n.$$

From this, the parameter in the exponential for the tail should be estimated as

$$\tau_0(Z) \sim \tau_0(\infty)[Z/(Z-1)]^{1/2}.$$

Figure 3 shows that the calculated tail decreases somewhat more steeply than the experimental one. This can show that the fluctuations of the longitudinal field in fact are attenuated to a smaller degree than in our calculation when the parameter $\nu=1/2$ is chosen, or rather that more neighbors should be included in the system of nonlinear equations. At the same time, we should point out that the correction terms added to Eq. (31), as shown by calculation, change the center of the spectrum, in particular the position of the maxima of the derivative, but have virtually no effect on the tail of the spectrum.

The resulting equations for the spin-system dynamics make it possible to describe other experiments as well as the NMR absorption spectra. As an example consider the experiment noted above, in which the rate of cross-polarization of an impurity of the rare isotope ^{43}Ca from the dipole–dipole reservoir of ^{19}F nuclei in a CaF_2 crystal is measured.[11] The dependence of the rate of this process on the rf field amplitude H_1 is determined by[11,31]

$$1/T_{IS}=M_{2IS}g(H_1)/\pi,$$

where M_{2IS} is the second moment at the impurity nucleus from the dipole interaction with the fluorine nuclei, and $g(H_1)$ is the spectrum of the correlation function of the longitudinal local field of Eq. (11) at the ^{43}Ca nucleus from the fluorine nuclei, normalized to unit area. As can be concluded from the values of the lattice sums,[12,31] the contribution with loops is even smaller in the [111] and [110] experimental field orientations than it was in the field at the ^{19}F nucleus. Therefore, $g(H_1)$ coincides with the spectrum of the correlation function $\Gamma_z(t)$ with high accuracy. The equation for calculating this function with the total second moment can be obtained from Eq. (29) after eliminating the division by $F_q(t')$ and adding in the brackets, in place of the subtractive term $b_q/F_q^2(t')$, the contribution $4(1-d_c)/9$ from distant spins. The functions $F_q(t)$ in this equation are calculated from the previous nonlinear equations. Because of the slow damping of $\Gamma_z(t)$, the time interval was increased to $40/M_2^{1/2}$ and broken up into 64 000 points. The results of the calculation of the spectra are shown in Fig. 4 along with the experimental data. A comparison shows that Eqs. (28) and (29) gave a good description of the cross-polarization and, consequently, of the fluctuations of the longitudinal local field. To be fair, it must be said that an equation with a Gaussian memory function[31] gave even better agreement. The reason is that the central part of the $\Gamma_z(t)$ spectrum, strongly narrowed by fluctuations, was in fact experimentally observed, as is evidenced by the large ratio of its moments, M_{4z}/M_{2z}^2. Therefore a self-consistent description of the fluctuations had no advantage over describing them by a Gaussian function, while a decrease appeared in M_{4z} because the interaction with distant spins was neglected in the nonlinear Eqs. (28)–(30).

We have thus convinced ourselves that the equations obtained here correctly describe the experiment in terms of cross-polarization and the tail of the NMR absorption line, measured by a continuous method. If we turn to the results in Fig. 1, obtained after Fourier-transforming the Engelsberg–Lowe formula, Eq. (1), for the falloffs of the free precession,

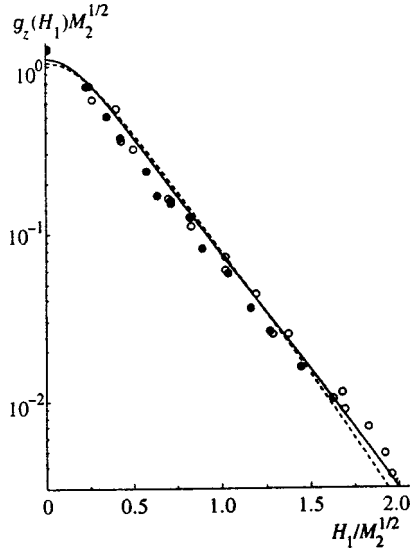

FIG. 4. Cross-polarization spectra for ^{43}Ca–^{19}F in CaF_2 for two magnetic field orientations. The experimental data of McArthur, Hahn, and Walstedt[11] are shown by the circles (open for $\mathbf{H}_0\|[111]$ and closed for $\mathbf{H}_0\|[110]$). The Fourier spectra of the correlation functions $\Gamma_z(t)$ are shown by a solid curve for $\mathbf{H}_0\|[111]$ and by a dashed curve for $\mathbf{H}_0\|[110]$.

we can conclude that this function gives a fairly good description of the tails of the spectra in the [100] and [111] orientations, but makes the decreasing tail in the [110] orientation appreciably steeper.

Let us now analyze the shape of the tail that follows from the theories cited above. The authors of Refs. 4 and 5 in general failed to take into account the fluctuations of the longitudinal local field, and therefore the tail of the NMR spectrum falls off even more steeply in their theory than does the tail of a Gaussian function. Reference 6 introduced a substantial improvement: Instead of considering the entire longitudinal local field to be unchanged, they considered the contribution to it from the close-lying spins (the spins of the cell) to be unchanged, while the field of the distant spins is described by a Gauss–Gauss random process. These changes brought the tail of the theoretical NMR spectrum closer to the experimental spectrum, but the description of the center of the spectrum became even worse. The approach in which a cell was distinguished was developed further in Ref. 9. However, since the contribution of the distant spins is introduced into the falloff of the free procession by multiplying by the exponential multiplier from the Engelsberg–Lowe function, Eq. (1), the same tail is obtained as in the spectrum of that function. Finally, Ref. 10 assumed that the longitudinal local field from all the spins fluctuated. A discontinuous Markov process is used to specify the field variations in time; this should work well for describing the changes of the NMR spectra, because of the mobility of the atoms and molecules.[25,32] This is by no means a successful approximation of the actual local-field fluctuations in a rigid lattice, since it gives a Lorentzian tail for the spectrum and consequently an infinite value for all the spectral moments, whereas they should have finite values in a rigid lattice.[25]

Another approach that does not use the concept of longitudinal local field was given in Ref. 8. In that paper, the

effect of the dipole–dipole interaction between the projections of the spins on the external magnetic field was mainly taken into account in a continued-fraction formalism. It was shown that, when the interaction between the transverse spin components is truncated in the dipole–dipole Hamiltonian, the coefficients in the continued fraction increase linearly as the number increases. When the truncated interaction is included, the increase of the coefficients accelerates. To obtain a closed expression that could be used for a calculation, the authors had to make an assumption concerning the form of this dependence. It was proposed to extrapolate the quadratic dependence on the number, established from the exact values of the first four coefficients. A similar dependence was detected earlier in the anisotropic Heisenberg model.[33] The unusual properties of continued fractions with such coefficients were discussed in Refs. 33 and 34. It is interesting for us that the tail of the spectrum is obtained as an exponential for such an approximation, in agreement with the result of our theory of a self-consistent fluctuating field. The formal transition in the continued fractions from a linear to a quadratic dependence of the coefficients on the number thereby obtained a physical explanation in our theory as a transition from constant local fields to fluctuating fields. To simplify the calculations, instead of a quadratic dependence, the same paper[8] later postulates that the coefficients, beginning with the fifteenth, are constant. In this case, a spectrum is obtained with truncated tails. The truncations, it is true, are rather far from the center.

This review of the work shows that the main advantage of the proposed theory over other theories is that, when the correlation functions are computed from self-consistent equations, it becomes unnecessary to postulate their shape or the shape of the memory function in the equations for them. Other advantages that made it possible to achieve better agreement with experiment are that the theory takes into account the finiteness of the number of nearest neighbors and polarization transfer via complex correlations. At the same time, the estimate of the attenuation of the field fluctuations still needs to be refined in order to more consistently take into account the contribution of the distant spins, as well as the contribution of complex loops.

5. CONCLUSION

Thus, both pulsed and continuous NMR studies have revealed that the tails of the spectrum have an exponential dependence. Varying the parameters of this dependence by changing the orientation of the crystal in a magnetic field does not alter the second moment of the spectrum. We explain this fact by means of nonlinear equations for the correlation functions, derived in the approximation of a self-consistent fluctuating field, taking into account the properties of the actual lattice. It has been shown that a tail of exponential shape results from self-consistent local-field fluctuations. The number of nearest neighbors and the contribution of the complex correlations change with orientation because of the anisotropy of the dipole–dipole interaction, and this changes the intensity of the local-field fluctuations and causes a dependence of the parameters of the tail in addition to that involving the second moment. On the other hand, if one restricts oneself to the approximation of constant local fields, one can arrive at the erroneous conclusion, drawn, for example, by Waugh,[35] that the spectrum will have a limit; if the rf field is detuned beyond this limit, the field ceases to heat the spin system. As shown above, this is not so. The spectrum, although exponentially weak, extends to virtually infinite frequencies. This conclusion is important for the theory of the establishment of equilibrium in spin systems.

The authors are grateful to P. P. Fedorov for providing a single crystal of BaF_2 and to V. A. Atsarkin, F. S. Dzheparov, and A. A. Lundin for discussing the results of the work.

This work was carried out with the financial support of the Krasnoyarsk Regional Science Fund (Grant 5F0068).

APPENDIX A

From the theory for computing the asymptotic forms of integrals,[36] the Fourier transform of the Engelsberg–Lowe function, Eq. (1), is determined for sufficiently large frequencies by its behavior on the imaginary time axis close to the branch point $t=iA$. In this region, we substitute the variable $t=i\tau$ and rewrite the product in the function in Eq. (1) in a new form:

$$\prod_{n=1}(1+\alpha_n^2\tau^2)=\frac{\sinh(b\tau)}{b\tau}\prod_{n=1}\frac{1+\alpha_n^2\tau^2}{1+\tau^2/(n\tau')^2}, \qquad \text{(A1)}$$

where the factors with the first nonequidistant zeros of the falloff of the free precession have been retained in the product, while the infinite product with equidistant zeros ($t_n=n\tau'$, a prime that was absent in Ref. 3 is added to prevent it from being confused with imaginary time) is collected into the function $\sin(bt)/bt$ (Ref. 3) with parameter $b=\pi/\tau'$. The product on the right-hand side of Eq. (A1) varies insignificantly on the interval $(iA, i\infty)$ of the imaginary axis of interest to us, and therefore we substitute into Eq. (A1) its value D at point $t=iA$ ($\tau=A$), which has the following values in the three orientations: 0.883 in [100], 0.514 in [110] and 0.690 in [111]. After this, the desired derivative of the spectrum is expressed in terms of the modified Bessel function of the second kind. Limiting ourselves to the first terms of the asymptotic series of this function, we get

$$\frac{d}{d\omega}g(\omega)\approx\frac{DC}{2b}\left(\frac{A}{2\pi}\right)^{1/2}\Omega^{-3/2}\exp\{A(C-\Omega)\}, \qquad \text{(A2)}$$

where

$$\Omega=[(\omega-b)^2+C^2]^{1/2}.$$

For $\omega=2M_2^{1/2}$, the value of Eq. (A2) is 15% less than the calculated spectrum of the function in Eq. (1), whereas, beginning with $2.5M_2^{1/2}$ it virtually coincides with it.

APPENDIX B

Let us determine the principal part of the solution of the system of Eqs. (28) and (29) in the neighborhood of the singular point with coordinate τ_0, using a method analogous

to the Painlevé analysis of the movable singularities of nonlinear ordinary differential equations. In order to do this, we write it in the form

$$F_q(t)\approx c_q(it+\tau_0)^{-\delta_q},\quad \Gamma_{z/q}(t)\approx a_q(it+\tau_0)^{-\zeta_q},\quad \text{(B1)}$$

substitute in Eqs. (28) and (29), and keep only the principal terms on the right-hand sides. From the condition of the equality of the left- and right-hand sides of the resulting equations, we find for the singularity indices

$$\begin{aligned}&\delta_1=\delta_2=\delta_3=2(1+\nu)/[\nu(2Z-3)-1],\\ &\zeta_1=\zeta_2=\zeta_3=(2+\delta_1)/\nu=\delta_1(2Z-3)-2,\end{aligned}\quad \text{(B2)}$$

while we get for the amplitudes a system of algebraic equations:

$$a_q\zeta_1(1+\zeta_1)=\frac{1}{2}\frac{c^2}{c_q}\left(\frac{n_1b_1}{c_1^2}+\frac{n_2b_2}{c_2^2}+\frac{n_3b_3}{c_3^2}-\frac{b_q}{c_q^2}\right),$$

$$\lambda^2 b_q a_q^{\nu}=c_q\delta_1(1+\delta_1),\quad c=c_1^{n_1}c_2^{n_2}c_3^{n_3}.$$

In the same way, for the characteristics of the function

$$\Gamma_z(t)\approx a(it+\tau_0)^{-\zeta}\quad \text{(B3)}$$

we find

$$\begin{aligned}&\zeta=\zeta_1+\delta_1=2(2Z-1+\nu)/[\nu(2Z-3)-1],\\ &a\zeta(1+\zeta)=\frac{c^2}{2}\left(\frac{n_1b_1}{c_1^2}+\frac{n_2b_2}{c_2^2}+\frac{n_3b_3}{c_3^2}\right).\end{aligned}\quad \text{(B4)}$$

Finally, if we substitute Eq. (B3) into Eq. (34), we find that the singularity in function $R_f(t)$ is stronger than in the other functions. To correct this disagreement, the power ν should be replaced by the smaller β, determined by the condition $\beta\zeta=2$. The reason is that changing the orientations of the spins far from the selected spin produces a smaller change of the local field than does the reorientation of the neighboring spins. In exactly the same way, ν should be replaced by β in the correction terms $\Phi_{2n}(t)$. We did not make these replacements in the text above, since they do not appreciably change the calculated curves in the regions under consideration.

*)E-mail: root@iph.krasnoyarsk.su

[1] V. E. Zobov, A. A. Lundin, Zh. Éksp. Teor. Fiz. **106**, 1097 (1994) [JETP **79**, 595 (1994)].
[2] C. R. Bruce, Phys. Rev. **107**, 43 (1957).
[3] M. Engelsberg and I. J. Lowe, Phys. Rev. B **10**, 822 (1974).
[4] K. W. Becker, T. Plefka, and G. Sauermann, J. Phys. C **9**, 4041 (1976).
[5] G. Sauermann and M. Wiegand, Physica B **103**, 309 (1981).
[6] G. E. Karnaukh, A. A. Lundin, B. N. Provotorov, and K. T. Summanen, Zh. Éksp. Teor. Fiz. **91**, 2229, (1986) [Sov. Phys. JETP **64**, 1324 (1986)].
[7] R. N. Shakhmuratov, J. Phys.: Condens. Matter **3**, 8683 (1991).
[8] J. Jensen, Phys. Rev. B **52**, 9611 (1995).
[9] A. A. Lundin, Zh. Éksp. Teor. Fiz. **110**, 1378 (1996) [JETP **83**, 759 (1996)].
[10] B. N. Provotorov, T. P. Kulagina, and G. E. Karnaukh, Zh. Éksp. Teor. Fiz. **113**, 967 (1998) [JETP **86**, 527 (1998)].
[11] D. A. McArthur, E. L. Hahn, and R. E. Walstedt, Phys. Rev. **188**, 609 (1969).
[12] H. T. Stokes and D. C. Ailion, Phys. Rev. B **15**, 1271 (1977).
[13] C. Cusumano and G. J. Troup, Phys. Status Solidi B **65**, 655 (1974).
[14] V. A. Atsarkin, G. A. Vasneva, and V. V. Demidov, Zh. Éksp. Teor. Fiz. **91**, 1523 (1986) [Sov. Phys. JETP **64**, 898 (1986)].
[15] M. Blume and J. Hubbard, Phys. Rev. B **1**, 3815 (1970).
[16] V. E. Zobov, Preprints 514F and 518F, Inst. Fiz. Sib. Otdel. Ross. Akad. Nauk, Krasnoyarsk (1988).
[17] V. E. Zobov, Teor. Mat. Fiz. **77**, 426 (1988); **84**, 111 (1990).
[18] A. A. Lundin, A. V. Makarenko, and V. E. Zobov, J. Phys.: Condens. Matter **2**, 10 131 (1990).
[19] V. E. Zobov, M. A. Popov, Teor. Mat. Fiz. **112**, 479 (1997).
[20] R. W. G. Wyckoff, *Crystal Structures*, vol. 1 (Wiley, New York, 1963).
[21] É. I. Fedin, I. K. Shmyrev, and A. I. Kitaĭgorodskiĭ, in *Paramagnetic Resonance* (Nauka, Moscow, 1971), p. 283.
[22] G. W. Canters and C. S. Johnson, Jr., J. Magn. Reson. **6**, 1 (1972).
[23] E. R. Andrew, Phys. Rev. **91**, 425 (1953).
[24] K. W. Vollmers, I. J. Lowe, and M. Punkkinen, J. Magn. Reson. **30**, 33 (1978).
[25] A. Abragam, *The Principles of Nuclear Magnetism* (Clarendon Press, Oxford, 1961; Inostr. Lit., Moscow, 1963).
[26] P. Borckmans and D. Walgraef, Physica (Amsterdam) **35**, 80 (1967); Phys. Rev. **167**, 282 (1968).
[27] P. Borckmans and D. Walgraef, Phys. Rev. B **7**, 563 (1973).
[28] M. I. Bulgakov, A. D. Gul'ko, F. S. Dzheparov *et al.*, JETP Lett. **58**, 592 (1993).
[29] P. W. Anderson and P. R. Weiss, Rev. Mod. Phys. **25**, 269 (1953).
[30] A. Lösche, *Kerninduktion* (Deutsche Verlag der Wissenschaften, Berlin, 1957; Inostr. Lit., Moscow, 1963).
[31] D. E. Demco, J. Tegenfeldt, and J. S. Waugh, Phys. Rev. B **15**, 4133 (1975).
[32] V. E. Zobov, in *The rf Spectroscopy of Solids*, Part 1 (Inst. Fiz. Sib. Otdel. Ross. Akad. Nauk, Krasnoyarsk, 1974), p. 22.
[33] M. Böhm, H. Leschke, M. Henneke *et al.*, Phys. Rev. B **49**, 417 (1994).
[34] M. H. Lee, J. Kim, W. P. Cummings, and R. Dekeyser, J. Phys.: Condens. Matter **7**, 3187 (1995).
[35] J. S. Waugh, in *NMR and More in Honour of Anatole Abragam*, Ed. M. Goldman and M. Porneuf (Les Editions de Physique Les Ulis, France,1994), p. 353.
[36] M. V. Fedoryuk, *Asymptotics: Integrals and Series* (Nauka, Moscow, 1987).

Translated by W. J. Manthey